Unfold: An integrated toolbox for overlap correction, non-linear modeling, and regression-based EEG analysis

Benedikt V. Ehinger [1*] & Olaf Dimigen [2]

[1] Institute of Cognitive Science, Universität Osnabrück

[2] Department of Psychology, Humboldt-Universität zu Berlin

Benedikt Ehinger (behinger@uos.de)
Wachsbleiche 27
49089 Osnabrück
Tel. +49 541 969-2245
Fax +49 541 969-2596

Olaf Dimigen (olaf.dimigen@hu-berlin.de)
Unter den Linden 6
10099 Berlin
Tel. +49 30 2093-4849
Fax +49 30 2093-4910

Author note: The authors would like to thank Bernhard Spitzer for helpful discussions about deconvolution models, as well as Peter König, Guang Ouyang, Ashima Keshava, and Scott Makeig for comments on earlier versions of this paper.

This article is a preprint that has not yet been peer-reviewed. It can be cited as: Ehinger, B.V. & Dimigen, O. (2018). Unfold: An integrated toolbox for overlap correction, non-linear modeling, and regression-based EEG analysis. *bioRxiv*. doi: https://doi.org/10.1101/360156. See also: https://www.biorxiv.org/content/early/2018/07/04/360156

ABSTRACT

Electrophysiological research with event-related brain potentials (ERPs) is increasingly moving from simple, strictly orthogonal stimulation paradigms towards more complex, quasi-experimental designs and naturalistic situations that involve fast, multisensory stimulation and complex motor behavior. As a result, electrophysiological responses from subsequent events often overlap with each other. In addition, the recorded neural activity is typically modulated by numerous covariates, which influence the measured responses in a linear or nonlinear fashion. Examples of paradigms where systematic temporal overlap variations and low-level confounds between conditions cannot be avoided include combined EEG/eye-tracking experiments during natural vision, fast multisensory stimulation experiments, and mobile brain/body imaging studies. However, even "traditional", highly controlled ERP datasets often contain a hidden mix of overlapping activity (e.g. from stimulus onsets, involuntary microsaccades, or button presses) and it is helpful or even necessary to disentangle these components for a correct interpretation of the results. In this paper, we introduce *unfold*, a powerful, yet easy-to-use MATLAB toolbox for regression-based EEG analyses that combines existing concepts of massive univariate modeling ("regression ERPs"), linear deconvolution modeling, and non-linear modeling with the generalized additive model (GAM) into one coherent and flexible analysis framework. The toolbox is modular, compatible with EEGLAB and can handle even large datasets efficiently. It also includes advanced options for regularization and the use of temporal basis functions (e.g. Fourier sets). We illustrate the advantages of this approach for simulated data as well as data from a standard face recognition experiment. In addition to traditional and non-conventional EEG/ERP designs, *unfold* can also be applied to other overlapping physiological signals, such as pupillary or electrodermal responses. It is available as open-source software at http://www.unfoldtoolbox.org.

Keywords: EEG, ERP, overlap correction, linear modeling of EEG, regression-ERP (rERP), generalized additive model (GAM), non-linear modeling, regression splines, regularization

INTRODUCTION

Event-related brain responses in the EEG are traditionally studied in strongly simplified and strictly orthogonal stimulus-response paradigms. In many cases, each experimental trial involves only a single, tightly controlled stimulation and a single manual response. In recent years, however, there has been rising interest in recording brain-electric activity also in more complex paradigms and naturalistic situations. Examples include laboratory studies with fast and concurrent streams of visual, auditory, and tactile stimuli (e.g. Spitzer et al., 2016), experiments that combine EEG recordings with eye-tracking recordings during natural vision (e.g. Dimigen et al., 2011), EEG studies in virtual reality (e.g. Ehinger et al., 2014) or mobile brain/body imaging studies that investigate real-world interactions of freely moving participants (e.g. Gramann et al., 2014). There are two main problems in these types of situations: Overlapping neural responses from subsequent events and complex influences of nuisance variables that cannot be fully controlled. However, even traditional ERP experiments often contain a mixture of overlapping neural responses, for example from stimulus onsets, involuntary microsaccades, or manual button presses.

Appropriate analysis of such datasets requires a paradigm shift away from simple averaging techniques towards more sophisticated, regression-based approaches (Amsel, 2011; Frömer, Maier, & Abdel Rahman, 2018; Hauk, Davis, Ford, Pulvermüller, & Marslen-Wilson, 2006; Pernet, Chauveau, Gaspar, & Rousselet, 2011; N. J. Smith & Kutas, 2015b; Van Humbeeck, Meghanathan, Wagemans, van Leeuwen, & Nikolaev, 2018) that can deconvolve overlapping potentials and also control or model the effects of both linear and non-linear covariates on the neural response. Importantly, the basic algorithms to deconvolve overlapping signals and to model the influences of both linear and non-linear covariates already exist. However, there is not yet a toolbox that integrates all of the necessary methods in one coherent workflow.

In the present paper we introduce *unfold*, an open source, easy-to-use, and flexible MATLAB toolbox written to facilitate the use of advanced deconvolution models and spline regression in ERP research. It performs these calculations efficiently even for large models and datasets and allows to run complex models with a few lines of codes. The toolbox is programmed in a modular fashion, meaning that intermediate analysis steps can be readily inspected and modified by the user if needed. It is also fully documented, can employ regularization, can model both linear and nonlinear effects using spline regression, and is compatible with EEGLAB (Delorme & Makeig, 2004) a widely used toolbox (Hanke &

Halchenko, 2011) to preprocess electrophysiological data that offers importers for many other biometric data formats, including eye-tracking and pupillometric data as well. *unfold* offers built-in functions to visualize the model coefficients (betas) of each predictor as waveforms or scalp topographies (i.e. "regression-ERPs", rERPS, Burns, Bigdely-Shamlo, Smith, Kreutz-Delgado, & Makeig, 2013; N. J. Smith & Kutas, 2015a). Alternatively, results can be easily exported as plain text or transferred to other toolboxes like EEGLAB or Fieldtrip (Oostenveld, Fries, Maris, & Schoffelen, 2011). For statistical analyses at the group level, that is second-level statistics, the resulting rERPs can be treated just like any other subject-level ERPs. As one suggestion, *unfold* integrates threshold-free cluster-based permutation tests for this purpose (Mensen & Khatami, 2013; S. M. Smith & Nichols, 2009)

In the following, we first briefly summarize some key concepts of regression-based EEG analysis, with an emphasis on linear deconvolution, spline regression, and temporal basis functions. We then describe the *unfold* toolbox that combines these concepts into one coherent framework. Finally, we illustrate its application to simulated data as well as real data from a standard ERP experiment. In particular, we will go through the typical steps to run and analyze a deconvolution model, using the data of a standard face recognition ERP experiment that contains overlapping potentials from three different sources: from stimulus onsets, from button presses, and from microsaccades that were involuntarily made by the participants during the task. We also give detailed descriptions of the features of the toolbox, including practical recommendations, simulation results, and advanced features such as regularization options or the use of temporal basis functions. We hope that our toolbox will both improve the understanding of traditional EEG datasets (e.g. by separating stimulus- and response-related components) as well as facilitate electrophysiological analyses in complex or (quasi-)natural situations, such as in combined eye-tracking/EEG and mobile brain/body imaging studies.

A simple simulation example

Before we introduce a real dataset, let us first consider a simulated simple EEG/ERP study to illustrate the possibilities of the deconvolution approach. For this, let's imagine a typical stimulus-discrimination task with two conditions (Figure 1): Participants are shown pictures of faces or houses and asked to classify the type of stimulus with a button press. Because this response is speeded, motor activity related to the preparation and execution of the manual response will overlap with the activity elicited by stimulus onset. Furthermore, we also assume that the mean reaction time (RTs) differs between the conditions, as it is the case in most experiments. In our example, if face pictures are on average classified faster than houses

pictures (Figure 1C), then a different overlap between stimulus- and response-related potentials will be observed in the two conditions. Importantly, as Figure 1F shows, this will result in spurious conditions effects due to the varying temporal overlap alone, and can be further mistaken for genuine differences in the brain's processing of houses and faces.

Faces are also complex, high-dimensional stimuli with numerous properties that are difficult to perfectly control and orthogonalize in any given study. For simplicity, we assume that the average luminance of the stimuli was not perfectly matched between conditions and is slightly, but systematically, higher for faces than houses (Figure 1D). From previous studies, we know that the amplitude of the P1 visually-evoked potential increases as a non-linear (log) function of the luminance of the presented stimulus (Halliday, 1982), and thus we also simulated a logarithmic effect of luminance on the P1 of the stimulus-aligned ERP (Figure 1E), creating another spurious condition difference (Figure 1G) in addition to that of varying response times (Figure 1F).

Panels G and H of Figure 1 show the same data modeled with *unfold*. Fortunately, with linear deconvolution modeling, we can not only remove the overlap effect (Figure 1G), but by including luminance as a non-linear predictor, we simultaneously also control the influence of this covariate (Figure 1H). How this is done is explained in more detail in the following.

Figure 1

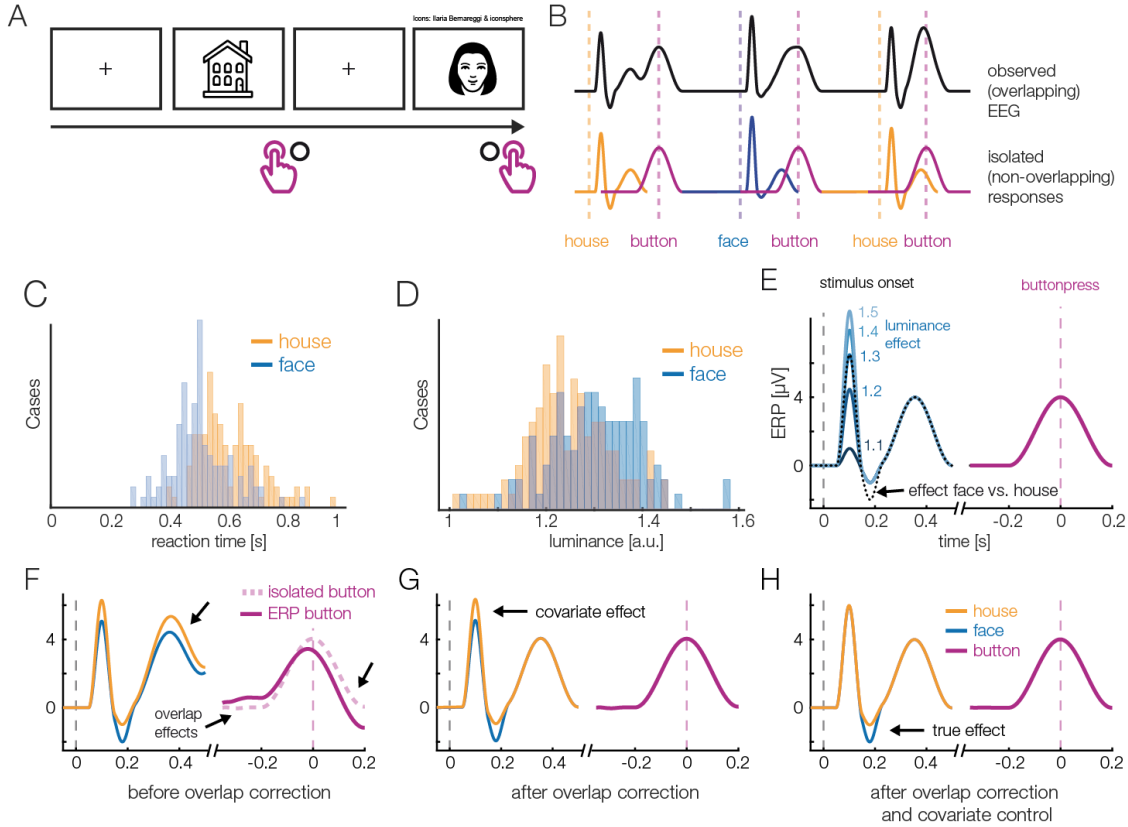

Figure 1. (A) A hypothetical simple ERP experiment with overlapping responses and a non-linear covariate. Data in this figure was simulated and then modeled with *unfold*. Participants saw pictures of faces or house and categorized them with a button press. (B) A short interval of the recorded EEG. Every stimulus onset and every button press elicits a brain response (lower row). However, because brain responses to the stimulus overlap with that to the response, we can only observe the sum of the overlapping responses in the EEG (upper row). (C) Because humans are experts for faces, we assume here that they reacted faster to faces than houses, meaning that the overlap with the preceding stimulus-onset ERP is larger in the face than house condition. (D) Furthermore, we assume that faces and house stimuli were not perfectly matched in terms of all other stimulus properties (e.g. spectrum, size, shape). For this example, let us simply assume that they differed in mean luminance. (E) The N170 component of the fERP is typically larger for faces than houses. In addition, however, the higher luminance alone increases the amplitude of the visual P1 component of the ERP. Because luminance is slightly higher for faces and houses, this will result in a spurious condition difference. (F) Average ERP for faces and houses, without deconvolution modeling. In addition to the genuine N170 effect (larger N170 for faces), we can see various spurious differences, caused by overlapping responses and the luminance difference. (G) Linear deconvolution corrects for the effects of overlapping potentials. (H) To also remove the confounding luminance effect, we need to also include this predictor in the model. Now we are able to only recover the true N170 effect without confounds (a similar figure was used in Dimigen & Ehinger, 2018).

Existing deconvolution approaches

Deconvolution methods for EEG have existing for some time (Hansen, 1983), but most older deconvolution approaches show severe limitations in their applicability. They are either restricted to just two different events (Hansen, 1983; Zhang, 1998), require special stimulus sequences (Delgado & Ozdamar, 2004; Eysholdt & Schreiner, 1982; Jewett et al., 2004; Marsh,

1992; Wang, Özdamar, Bohórquez, Shen, & Cheour, 2006), rely on semi-automatic, iterative methods like ADJAR (Woldorff, 1993) that can be slow or difficult to converge (Kristensen, Rivet, & Guérin-Dugué, 2017; Talsma & Woldorff, 2004), or were tailored for special applications. In particular, the specialized RIDE algorithm (Ouyang, Herzmann, Zhou, & Sommer, 2011; Ouyang, Sommer, & Zhou, 2015) offers a unique feature in that it able to deconvolve time-jittered ERP components even in the absence of a designated event marker. However, while RIDE has been successfully used to separate stimulus- and response-related ERP components (Ouyang et al., 2011, 2015); it does not support continuous predictors and is intended for a small number of overlapping events.

In recent years, an alternative deconvolution method based on the linear model has been proposed and successfully applied to the overlap problem (Bardy, Van Dun, Dillon, & Cowan, 2014; Dandekar, Privitera, Carney, & Klein, 2012; Kristensen, Guerin-Dugué, & Rivet, 2017; Kristensen, Rivet, et al., 2017; Litvak, Jha, Flandin, & Friston, 2013; Lütkenhöner, 2010; N. J. Smith & Kutas, 2015b; Spitzer, Blankenburg, & Summerfield, 2016). This deconvolution approach was first applied extensively to fMRI data (Dale & Buckner, 1997) where the slowly varying BOLD signal overlaps between subsequent events. However, in fMRI, the shape of the BOLD response is well-known and this prior knowledge allows the researcher to use model-based deconvolution. If no assumptions about the response shape (i.e. the kernel) are made, the approach used in fMRI is closely related to the basic linear deconvolution approach discussed below.

Deconvolution within the linear model

With deconvolution techniques, overlapping EEG activity is understood as the linear convolution of experimental event latencies with isolated neural responses (Figure 1B). The inverse operation is deconvolution, which recovers the unknown isolated neural responses given only the measured (convolved) EEG and the latencies of the experimental events (Figure 1H). Deconvolution is possible if the subsequent events in an experiment occur with varying temporal overlap, in a varying temporal sequence, or both. In classical experiments, stimulus-onset asynchronies and stimulus sequences can be varied experimentally and the latencies of motor actions (such as saccades or button presses) also vary naturally. This varying overlap allows for modeling of the unknown isolated responses, assuming that the overlapping signals add up linearly. More specifically, we assume (1) that the electrical fields generated by the brain sum linearly (a justified assumption, see Nunez and Srinivasan, 2009) and (2) that the

overlap, or interval between events, does not influence the computations occurring in the brain – and therefore the underlying waveforms (see also *Discussion*).

The benefits of this approach are numerous: The experimental design is not restricted to special stimulus sequences, multiple regression allows modeling of an arbitrary number of different events, and the mathematical properties of the linear model are well understood.

Figure 2

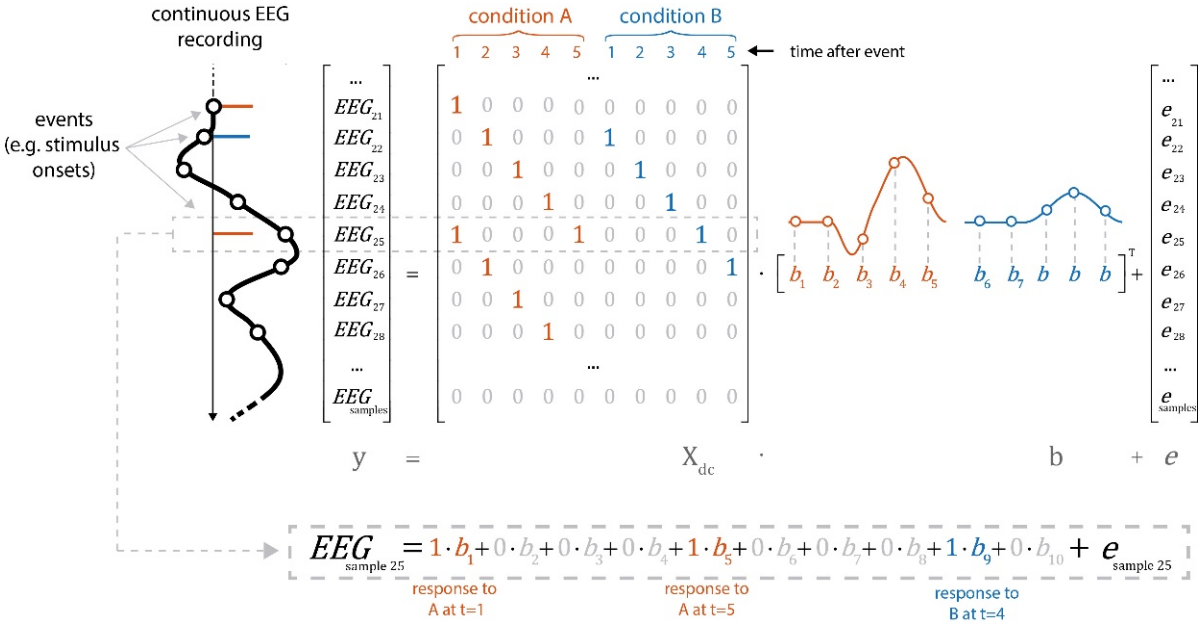

Figure 2. Linear deconvolution explains the continuous EEG signal within a single regression model. Specifically, we want to estimate the response (*betas*) evoked by each event so that together, they best explain the observed EEG. For this purpose, we create a *time-expanded* version of the design matrix (X_{dc}) in which a number of time points around each event (here: only 5 points) are added as predictors. We then solve the model for *b*, the betas. For instance, in the model above, sample number 25 of the continuous EEG recording can be explained by the sum of responses to three different experimental events: the response to a first event of type "A" (at time point 5 after that event), by the response to an event of type "B" (at time 4 after that event) and by a second occurrence of an event of type "A" (at time 1 after that event). Because the sequences of events and their temporal distances vary throughout the experiment, it is possible to find a unique solution for the betas that best explains the measured EEG signal. These betas, or "regression-ERPs" can then be plotted and analyzed like conventional ERP waveforms. Figure adapted from Dimigen & Ehinger, 2018 (with permission).

Linear deconvolution

The classic massive univariate linear model, *without* overlap correction, is applied to epoched EEG data and can be written as:

$$\mu_{i,\tau} = X_i \beta_\tau \; with \; y_{i,\tau} \sim normal(\mu_{i,\tau}, \sigma_\tau)$$

Here, X is the design matrix. It has i rows (each describing one instance of an event of type e) and c columns (each describing the status of one predictor).

Furthermore, let τ be the "local time" relative to onset of the event (e.g. -100 to +500 sampling points). $\mu_{i,\tau}$ is the EEG signal measured after event i that we wish to predict at a given time point τ relative to the event onset. β is a vector of unknown parameters that we wish to estimate for each time point in the epoched EEG data. Importantly, therefore, this approach fits a separate linear model at each time point τ.

A single entry will be referred by lowercase $x_{i,c}$.

In contrast, with linear deconvolution we enter the continuous EEG data into the model. We then make use of the knowledge that each observed sample of the continuous EEG can be described as the linear sum of (possibly) several overlapping event-related EEG responses. Depending on the latencies of the neighboring events, these overlapping responses occur at different times τ relative to the current event (see Figure 2). That is, in the example in Figure 2, where the responses of two types of events, A and B overlap with each other, the observed continuous EEG at time point t of the continuous EEG recording can be described as follows:

$$EEG_t = 1\beta_{A,1} + 0\beta_{A,2} + 0\beta_{A,3} + 0\beta_{A,4} + 1\beta_{A,5} + 0\beta_{B,1} + 0\beta_{B,2} + 0\beta_{B,3} + 1\beta_{B,4} + 0\beta_{B,5}$$

In the example in Figure 2, the spontaneous EEG at time-point t is modeled as the linear sum of a to-be-estimated response to the first instance of event type A at local time $\tau = 5$ (i.e. from the point of view of $EEG(t)$ this instance occurred 5 time samples before). Another response to the second instance of event type A at local time $\tau = 0$ (i.e. this instance just occurred at t), and another response to the instance of event type B at local time $\tau = 4$.

The necessary design matrix to implement this model, X_{dc}, will span the duration of the entire EEG recording. It can be generated from any design matrix X by an algorithm we will call *time expansion* in the following. In this process, each predictor in the original design matrix will be expanded to several columns, which then code a number of "local" time points relative to the event onset. An example for a time-expanded design matrix is shown in Figure 2.

Time expansion

The process to create the time-expanded design matrix X_{dc} is illustrated in Figure 2. In the following sections, we will describe the construction of X_{dc} more formally. Readers not interested in these technicalities may skip to the following section on non-linear effects.

Let t be the time of the continuous EEG signal y, which keeps increasing throughout the experiment. τ is still the local time, that is the temporal distance of an EEG sample relative to an instance of event e. Let i be the instance of one such event. X_i is therefore the accompanying

row of the design matrix X which specifies the predictors for each event of type e. The design matrix X consists of multiple columns c, each representing one predictor (for which we want to estimate the accompanying β).

X_{dc} can be constructed from multiple concatenated, time-shifted square diagonal matrices G with size τ one for each instance of the event e. For the purpose of illustration, it is helpful to construct the design matrix first for just a single predictor and a single instance of a single type of event (e.g. a manual response). Afterwards, we will add multiple predictors, then multiple instances of a single event type and finally multiple different event types (e.g. stimuli and responses).

Single predictor, single instance, single event type

The matrix G_c for a single predictor, single type of event, and single instance of this event type is square diagonal where the size is specified by the number of samples around the event instance onsets to be taken into account:

$$G_c = Ix_{i,c} = \begin{bmatrix} x_{i,c} & 0 & 0 & 0 \\ 0 & x_{i,c} & 0 & 0 \\ 0 & 0 & x_{i,c} & 0 \\ 0 & 0 & 0 & x_{i,c} \end{bmatrix}$$

It is a scaling of an identity matrix by the scalar $x_{i,c}$ which is a single entry of the design matrix X defining the predictor c at the single instance i. In the case of a dummy-coded variable (0 or 1) we would get either a matrix full of zeros or the identity matrix; in case of a continuous predictor we get a scalar matrix where the diagonal of $G_{i,c}$ contains the continuous predictor value.

Multiple predictors, single instance, single event type

In case of multiple predictors c, we generate multiple matrices $G_{i,c}$ and concatenate them to $G^* = [G_1 \dots G_c]$. Therefore, a matrix with two predictors at the instance i of an event e could look like:

$$G^* = [G_1 G_2] = \begin{bmatrix} 1 & 0 & 0 & 0 & 10 & 0 & 0 & 0 \\ 0 & 1 & 0 & 0 & 0 & 10 & 0 & 0 \\ 0 & 0 & 1 & 0 & 0 & 0 & 10 & 0 \\ 0 & 0 & 0 & 1 & 0 & 0 & 0 & 10 \end{bmatrix}$$

Multiple predictors, multiple instances, single events type

In case of multiple instances of the same event, we have one G^* matrix for every instance. We combine them into a large matrix X_{dc} by inserting the G^* matrices into X_{dc} around the time points (in continuous EEG time t) where the instance of the event occurred. Because τ (and therefore G^*) is usually larger than the time distance between two event instances, we insert rows of multiple G^* matrices in an overlapping (summed) way. Consequently, we model the same time point of the EEG by the combined rows of multiple G^* matrices (Figure 2, Figure 3A). By solving the linear system with $X_{dc}\beta$ for β we effectively deconvolve the original signal.

Multiple predictors, multiple instances, multiple events types

We usually have multiple different types of events $e_1, e_2 \ldots$. For each of these event types, we create one X_{dc}^e matrix as described above. Each X_{dc}^e matrix spans t rows and thus, the continuous EEG signal. To get the final matrix X_{dc} we simply concatenate them along the columns before the model inversion.

$$X_{dc} = [X_{dc}^1 \ldots X_{dc}^e]$$

Similarly, if we wanted to include a continuous covariate spanning the whole duration of the continuous EEG signal (see *Discussion),* for example some feature of a continuous audio signal (e.g. Crosse, Di Liberto, Bednar, & Lalor, 2016) we could simply concatenate it as an additional column to the design matrix.

The formula for the deconvolution model is then:

$$\mu_t = X_{dc,t}\,\beta \;\; with\; y_t \sim normal(\mu_t, \sigma)$$

μ_t is the expected value of the continuous EEG signal y_t. This time-expanded linear model simultaneously fits all the parameters β describing the deconvolved rERPs of interest. This comes at the cost of a very large (size: *number of samples* × *number of predictor columns*). Fortunately, this matrix is also very sparse, containing mostly zeros, and can therefore be efficiently solved with modern sparse solvers. For further detail see the excellent tutorial reviews by Smith and Kutas (N. J. Smith & Kutas, 2015a, 2015b).

Modeling non-linear effects with spline regression

Now we will outline how we can use spline predictors to model nonlinear effects within the linear regression framework. We follow the definition of a Generalized Additive Model (GAM) by Wood, (2017, p. 249-250):

$$\mu_i = X_i\beta + \sum_j z_j f_j(x_i)$$

The sum $\sum_j z_j f_j(x_i)$ represents a basis set with j unknown parameters z (analog to the β vector). The time-indices were omitted here. The most common example for such a basis set would be polynomial expansion. Using the polynomial basis set with order three would results in the following function:

$$\mu_i = X_i\beta + z_1x^1 + z_2x^2 + z_3x^3$$

However, due to several suboptimalities of the polynomial basis (e.g. Runge, 1901) we will make use of the cubic B-spline basis set instead. Spline regression is conceptually related to the better-known polynomial expansion, but instead of using polynomials, one uses locally bounded functions. In other words, whereas a polynomial ranges over the whole range of the continuous predictor, a B-spline is restricted to a local range.

This basis set is constructed using the De-Casteljau algorithm (De Casteljau, 1959) implemented by Bruno Luong (Luong, 2016). It is a basis set that is strictly local: Each basis function is non-zero only over a maximum of 5 other basis functions (for cubic splines; see Woods 2017, p. 204).

Multiple terms can be concatenated, resulting in a GAM:

$$\mu_i = X_i\beta + \sum_j z_j f_j(x_{1i}) + \sum_j z_j f_j(x_{2i})$$

If interactions between two non-linear spline predictors are expected, we can also make use of two-dimensional splines:

$$\mu_i = X_i\beta + \sum_j z_j f_j(x_{1i}, x_{2i})$$

In the *unfold* toolbox, 2D-splines are created based on the pairwise products between $z_{1,j}$ *and* $z_{2,j}$. Thus, a 2D spline between two spline-predictors with 10 spline-functions each would result in 100 parameters to be estimated.

The number of basis functions to use for each non-linear spline term are usually determined by either regularization or cross-validation. Cross-validation is difficult in the case of large EEG datasets (see also *Discussion*) and we therefore recommend to determine the number of splines (and thus the flexibility of the non-linear predictors) prior to the analysis to avoid overfitting.

Using temporal basis functions

In the previous section, we made use of time-expansion to model the overlap. For this, we used the so-called stick function approach (also referred to as FIR or dummy-coding). That is, each time-point relative to an event (local time) was coded using a 1 or 0 (in case of dummy-coded variables), resulting in a staircase patterns in the design matrix (cf. Figures 2 and 3A). However, this approach is computationally expensive. Due to the high sampling rate of EEG (typically 200-1000 Hz), already a single second of estimated ERP response requires us to estimate 200-1000 coefficients per predictor. Therefore, some groups started to use other time basis sets to effectively smooth the estimated regression-ERPs (e.g. Litvak et al., 2013; but see N. J. Smith & Kutas, 2015b).

We will discuss two examples here: The time-Fourier set (Litvak et al., 2013; Spitzer et al., 2016) and – newly introduced in this paper – the time-spline set. In the time-spline set, adjacent local time coefficients are effectively combined according to a spline set (Figure 3B). Splines are a suitable basis function because EEG signals are smooth and values close in time have similar values. The number of splines chosen here defines the amount of smoothing of the resulting deconvolved ERP. The same principle holds for the time-Fourier set. Here we replace the stick-function set with a truncated Fourier set (Figure 3C). Truncating the Fourier set at high frequencies effectively removed high frequencies from the modeled ERP and can therefore be thought of as a low-pass filter (see also Figure 6). A benefit of using temporal basis functions rather than the simple stick functions is that less unknown parameters need to be estimated. It is therefore possible that this results in numerical more stable solutions to the linear problem; however, we are also constraining the solution space.

Figure 3

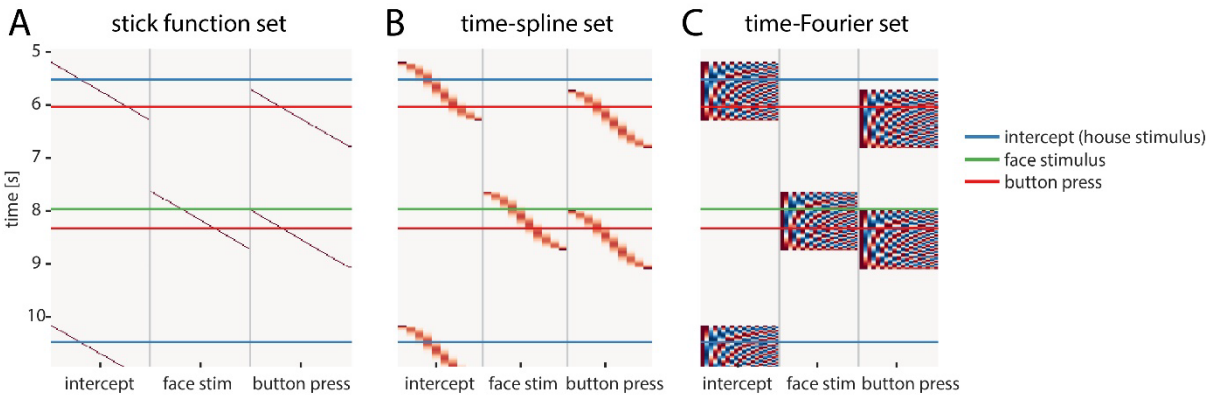

Figure 3. Overview over different temporal basis functions. The expanded design matrix X_{dc} is plotted, the y-axis represents time and the x-axis shows all time-expanded predictors in the model. In *unfold*, three methods are available for time expansion: (A) Stick-functions. Here, each modeled time point relative to the event is represented by a unique predictor. (B) Time-splines allow neighboring time points to smooth themselves. This generally results in less predictors than the stick function set. (C) Time-Fourier set: It is also possible to use a Fourier basis. By omitting high frequencies from the Fourier-set, the data are effectively low-pass filtered during the deconvolution process (see also Figure 6).

Existing toolboxes

To our knowledge, no existing toolbox supports non-linear, spline-based general additive modeling of EEG activity. Also, we were missing a toolbox that solely focuses on deconvolving signals and allowed for a simple specification of the model to be fitted, for example using the commonly used Wilkinson notation (as also used for example in *R*).

A few other existing EEG toolboxes allow for deconvolution analyses, but we found that each has their limitations. Plain linear modeling (including second-level analyses) can be performed using the LIMO toolbox (Pernet et al., 2011), but this toolbox does not support deconvolution analyses or spline regression. To our knowledge, four toolboxes support some form of deconvolution: SPM (Litvak et al., 2013; Penny, Friston, Ashburner, Kiebel, & Nichols, 2006), the rERP extension for EEGLAB (Burns et al., 2013), pyrERP (N. J. Smith, 2013), mTRF (Crosse et al., 2016) and MNE (Gramfort et al., 2014) . SPM allows for deconvolution of linear responses using Fourier temporal basis sets. However, in order to make use of these deconvolution functions, quite a bit of manual coding is needed. The rERP extension for EEGLAB and the pyrERP toolbox for Python both allow for estimation of linear models and deconvolution; however, both toolboxes appear not to be maintained anymore; rERP is currently non-functional (for current MATLAB versions) and no documentation is

available for pyERP. The MNE toolbox is a general-purpose Python-based EEG processing toolbox that allows for both deconvolution and massive univariate modeling. It is actively maintained and some basic tutorials are available. The mTRF toolbox is a special type of deconvolution toolbox designed to be used with continuous predictors (e.g. auditory streams) that last over the whole continuous EEG recording (see *Discussion*).

THE UNFOLD TOOLBOX

In the following, we describe basic and advanced features available in the *unfold* toolbox and also give practical recommendations for problems that researchers might experience in the modeling process. Specifically, we describe how to (1) specify the model via Wilkinson formulas, (2) include nonlinear predictors via spline regression, (3) model the data with basis functions over time (e.g. a Fourier basis set), (4) impute missing data in the design matrix, (5) treat intervals of the continuous EEG containing EEG artifacts (e.g. from muscle activity or skin conductance changes), (5) specify alternative solvers (with regularization) that can solve even large models in a reasonable time and (6) run the same regression model both as a deconvolution model and also a mass multivariate model without deconvolution. Finally, we summarize options for (7) visualizing and (8) exporting the results.

Data import

As a start, we need a data structure in EEGLAB format (Delorme & Makeig, 2004) that contains the continuous EEG data and event codes. In traditional EEG experiments, events will typically be stimulus and response triggers, but many other types of events are also possible (e.g., voice onsets, the on- or offsets of eye or body movements etc.). In most cases, the EEG data entered into the model should have already been corrected for biological and technical artifacts (e.g. ocular artifacts, scalp muscle EMG, or power line noise), for example with independent component analysis (ICA).

Figure 4

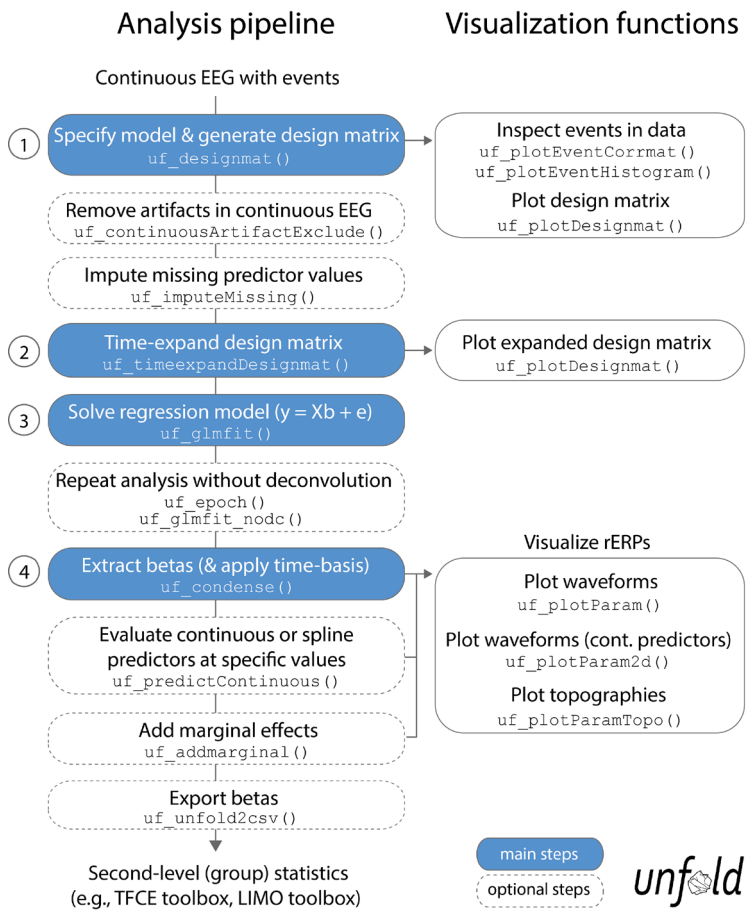

Figure 4. Overview over typical analysis steps with *unfold*. The first step is to load a continuous EEG dataset into EEGLAB. This dataset should already contain event markers (e.g. for stimulus onsets, button presses etc.). Afterwards there are four main analysis steps, that can be executed with a few lines of code (see also Box 1). These steps, highlighted in blue, are: (1) Define the model formula and let *unfold* generate the design matrix, (2) time-expand this design matrix, (3) solve the model to obtain the betas (i.e. rERPs), and (4) convert the betas into a convenient format for plotting and statistics. The right column lists several inbuild plotting functions to visualize intermediate analysis steps or to plot the results (see also Figure 8).

Specifying models using Wilkinson notation

We begin by the modeling process by specifying the model formula and by generating the corresponding design matrix X. In the *unfold* toolbox, models are specified using the intuitive Wilkinson notation (Wilkinson & Rogers, 1973) also commonly used in *R*, the Matlab statistics toolbox, and python StatsModels. For example, for the hypothetical face/house experiment depicted in Figure 1, we might define the following model:

```
EEG ~ 1 + cat(is_face) + luminance
```

More generally, we can also specify more complex formulas, such as:

```
EEG ~ 1 + cat(predictor1) + predictor2 + spl(predictor3)
```

Here, `cat()` specifies that the `predictor1` should be dummy encoded as a categorical variable or factor rather than treated as a continuous variable. If a variable is already dummy-coded as 0/1 it is not strictly necessary to add the `cat()` command, but it is also possible to specify multi-level categorical variables. In contrast, `predictor2` should be modeled as continuous linear covariate and `predictor3` as a nonlinear spline predictor. In the formula, a + sign means that only the main effects will be modeled. Interactions between predictors are added by replacing the + with a * or a `:`, depending on whether all main effects and interactions should be modeled (*), or only the interactions (`:`). In *unfold*, the type of coding (dummy/treatment/reference or effect/contrast/sum coding) can be selected. If the default treatment coding is used, the predictors will represent the difference to the intercept term (coded by the 1). The reference level of the categorical variable and the ordering of the levels is determined alphabetically or can be specified by the user manually. The toolbox also allows to specify different formulas for different events. For example, stimulus onset events can have a different (e.g. more complex) formula than manual response events.

Once the formula is defined, the design matrix X is time-expanded to X_{dc} and now spans the duration of the entire EEG recording. Subsequently, for each channel, the equation ($EEG = X_{dc} * b + e$) is solved for "b", the betas, which correspond to subject-level rERP waveforms. For example, in the model above, for which we used treatment coding, the intercept term would correspond to the group-average ERP. The other betas, such as those for `cat(is_face)`, will capture the partial effect of that particular predictor, corresponding to a difference wave in traditional ERPs (here: face-ERP minus house-ERP).

In the same linear model, we can simultaneously model brain responses evoked by other experimental events, such as button presses. Each of these other event types can be modeled by its own formula. In our face/house example, we would want to model the response-related ERP that is elicited by the button press at the end of the trial, because this ERP will otherwise overlap to a varying degree with the stimulus-ERP. We do this by defining an additional simple intercept model for all button press events. In this way, the ERP evoked by button presses will be removed from the estimation of the stimulus ERPs. The complete model would then be:

`EEG ~ 1 + cat(is_face) + spl(luminance,10)` {for stimulus onset events}

`EEG ~ 1` {for manual button press events}

Spline regression to model (nonlinear) predictors

As explained earlier, many influences on the EEG are not strictly linear. In addition to linear terms, one can therefore use cubic B-splines to perform spline regression, an approach commonly summarized under the name GAM (generalized additive modeling). An illustration of this approach is provided in Figure 5. In the *unfold* toolbox, spline regression can be performed by adding `spl()` around the predictor name, as for `predictor 3` in the formula above, which specifies a model using 10 B-splines instead of a continuous linear predictor. We can model covariates as non-linear predictors:

```
EEG ~ 1 + spl(A,10) + 2dspl(B,C,10) + circspl(D,10,0,360)
```

With this formula, the effect "A" would be modeled by a basis set consisting of ten splines. We would also fit a 2D spline between continuous variable B and C with ten splines each. In addition, we would fit a circular spline based on covariate D using ten splines with the limits 0° and 360° being the wrapping point of the circular spline.

Figure 5

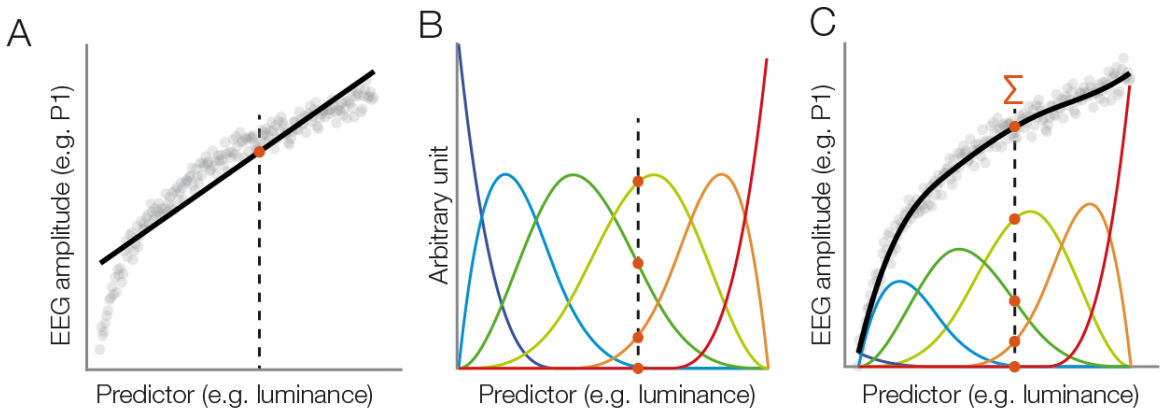

Figure 5. Modeling a nonlinear relationship with a set of spline functions. (A) Example of a non-linear relationship between a predictor (e.g. stimulus luminance) and a dependent variable (e.g. EEG amplitude). A linear function (black line) does not fit the data well. We will follow one luminance value (dashed line) at which the linear function is evaluated (red dot). (B) Instead of a linear fit, we define a set of overlapping spline functions which are distributed across the range of the predictor. In this example, we are using a set of six b-splines. For our luminance value, we receive six new predictor values. Only three of them are non-zero. (C) We weight each spline with its respective estimated beta value. To predict the dependent variable (EEG amplitude) at our luminance value (dashed line), we sum up the weighted spline functions (red dots). Because the splines are overlapping, this produces a smooth, non-linear fit to the observed data.

In *unfold*, three spline functions are already implemented. For B-splines we use the de Casteljau algorithm implemented by Bruno Luong. For interactions between spline-modeled covariates, first the default spline function is used on each predictor to generate n splines. Then the resulting vectors are elementwise multiplied with each other, generating n^2 final predictors. For cyclical predictors such as the angle of a saccadic eye movement (which ranges e.g. from 0 to 2π), it is possibly to use cyclical B-splines, as explained above. These are implemented based on code from *patsy*, a python statistical package (https://patsy.readthedocs.io) which follows an algorithm described in Woods (Wood, 2017, pp. 201-205). For maximal flexibility, we also allow the user to define custom spline functions. This would also allow to implement other basis sets, for example polynomial expansion.

The placement of knots and the number of splines used are critical parameters to appropriately model the predictor and to avoid over- or underfitting the data. The toolbox's default knot placement is on the quantiles of the predictor. This can be changed by users who want to use a custom sequence of knots. Generalized cross validation could be used to narrow down the number of knots to be used.

Figure 6

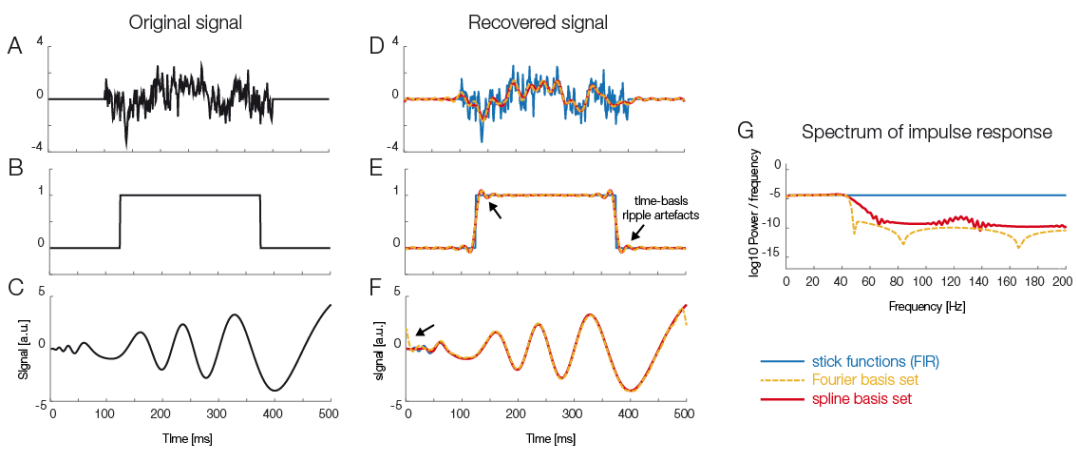

Figure 6. Using temporal basis functions. Effect of using different time basis functions on the recovery of the original signal using deconvolution. Panels A, B, and C show three different example signals without deconvolution (in black) and with convolution using different methods for the time-expansion (stick, Fourier, spline). We zero-padded the original signal to be able to show boundary artefacts. For the analysis we used 45 time-splines and in order to keep the number of parameters equivalent, the first 22 cosine and sine functions of the Fourier set. The smoothing effects of using a time-basis set can be best seen in the difference between the blue curve and the orange/red curves in panel D. Artefacts introduced due to the time-basis set are highlighted with arrows and can be seen best in panels E and F. Note that in the case of realistic EEG data, the signal is typically smooth, meaning that ripples like in panel E rarely

occur. (G) The impulse response spectrum of the different smoothers. Clearly, the Fourier-set filters better than the splines, but splines allow for a sparser description of the data and could benefit in the fitting stage.

Using time basis functions

Temporal basis functions were introduced earlier. The stick-function approach, as also illustrated in Figures 2 and 3A is the default option in *unfold*. As alternatives, it is also possible to employ either a Fourier basis set or a set of *temporal* spline function. For example, for the time-expansion step, Litvak and colleagues (Litvak et al., 2013; Spitzer et al., 2016) used a Fourier basis sets instead of stick-functions. Figure 6 compares simulation results for stick functions with those obtained with a Fourier basis set and a spline basis set in terms of the spectral components and the resulting filter artifacts. At this point, more simulation studies are needed to understand the effects of temporal basis sets on EEG data. We therefore follow the recommendation of Smith & Kutas (N. J. Smith & Kutas, 2015b) to use stick-functions for now.

Imputation of missing values

In multiple regression models it is typically necessary to remove the whole trial if one of the predictors has a missing value. One workaround for this practical problem is to impute (i.e. interpolate) the value of missing predictors. In the deconvolution case, imputation is even more important for a reliable model fit, because if a whole event is removed, then overlapping activity from this event with that of the neighboring events would not be accounted for. In *unfold* we therefore offer several algorithms to treat missing values: the dropping of events with missing information, or imputation by the marginal, mean, or median values of the other events.

Dealing with EEG artifacts

Linear deconvolution needs to be performed on continuous, rather than epoched data. This creates challenges with regard to the treatment of intervals that contain EEG artifacts. The way to handle artifacts in a linear deconvolution model is therefore to detect – but not to remove – the intervals containing artifacts in the continuous dataset. For these contaminated time windows, the time-expanded design matrix (X_{dc}) is then blanked out, that is, filled with zeros, so that the artifacts do not affect the model estimation (N. J. Smith & Kutas, 2015b).

Of course, this requires the researcher to use methods for artifact correction that can be applied to continuous rather than segmented data (such as ICA). Similarly, we need methods

that can detect residual artifacts in the continuous rather than epoched EEG. One example would be a peak-to-peak voltage threshold that is applied within a moving time window that is shifted step-by-step across the entire recording. Whenever the peak-to-peak voltage within the window exceeds a given threshold, the corresponding interval would then be blanked out in the design matrix. Detecting artifacts in the continuous rather than segmented EEG also has some small additional benefit, because if the data of a trial is only partially contaminated, the clean parts can still enter the model estimation (N. J. Smith & Kutas, 2015b).

The *unfold* toolbox includes a function to remove artefactual intervals from the design matrix before fitting the model. In addition, we offer basic functionality, adapted from ERPLAB (Lopez-Calderon & Luck, 2014), to detect artifacts in the continuous EEG.

Multiple solvers: LSMR & glmnet

Solving for the betas is not always easy in such a large model. We offer several algorithms to solve for the parameters. The currently recommended one is LSMR (Fong & Saunders, 2011), an iterative algorithm for sparse least-squares problems. This algorithm allows to use very large design matrices as long as they are sparse (i.e. contain mostly zeroes) which is usually the case if one uses time-expansion based on stick-functions (cf. Figures 2 and 3A).

However, especially with data containing a high level of noise, the tradeoff between bias and variance (i.e. between under- and overfitting) might be suboptimal, meaning that the parameters estimated from the data might be only weakly predictive for held-out data (i.e. they show a high variance and tend to overfit the data). The *unfold* toolbox therefore allows the user to specify alternative solvers that use regularization. In particular, we include the *glmnet*-solver (Qian, Hastie, Friedman, Tibshirani, & Simon, 2013), which allows for ridge (L2-norm), lasso (L1, leads to sparse solutions) and elastic net regularization. The regularization parameter is automatically estimated using cross-validation. Procedures to regularize with linear deconvolution have recently been examined and validated by Kristensen et al. (2017a). Effects of regularization on noisy data are also depicted in Figure 7, which compares deconvolution results for noisy simulated data with and without regularization. As can be seen in this figure, the non-regularized estimates show strong variance (panel B and C), whereas the regularized estimates show strong bias (panel D and E), that is, the estimated effects are shrunk towards zero but simultaneously, the variance of the estimate over time is greatly reduced. At this point, it is not yet clear whether and how much regularization should be used for the standard analysis

of EEG data, but we provide different solvers in *unfold* to facilitate future work on this topic. Please also see Kristensen et al. (2017a) for more simulation work.

Figure 7

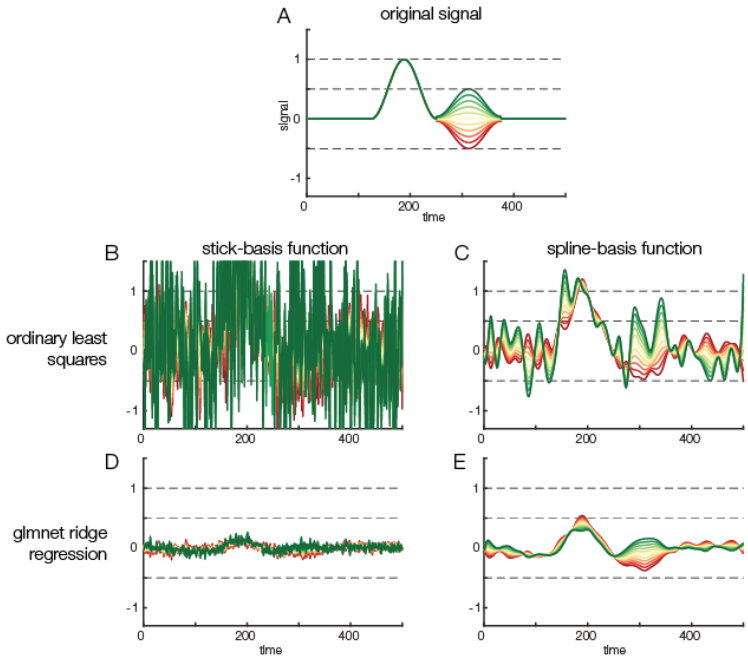

Figure 7. Regularization options. Effects of regularization on deconvolving noisy data. Results of regularization are shown both for a model with stick-functions and for a model with a temporal spline basis set. (A) To create an overlapped EEG signal, we convolved 38 instances of the original signal depicted in panel A. The effect of a continuous covariate was randomly added to each event (see different colors in A). To make the data noisy, we added Gaussian white noise with a standard deviation of 1. Finally, to illustrate the power of regularization, we also added another random covariate to the model. This covariate had no relation to the EEG signal but was highly correlated ($r = 0.85$) to the first covariate. Thus, the model formula was: `EEG ~ 1 + covariate + randomCovariate`. (B) Parameters recovered based on ordinary least squares regression. Due to the low signal-to-noise ratio of the data, the estimates are extremely noisy. (C) Some smoothing effect can be achieved by using time-splines as a temporal basis set instead of stick functions. (D) The same data, but deconvolved using a L2-regularized estimate (ridge regression). It is obvious that the variance of the estimate is a lot smaller. However, compared to the original signal shown in panel A, the estimated signal is also much weaker, i.e. there is a strong bias. (E) L2-regularized estimates, computed with a time-spline basis set. This panel shows the usefulness of regularization: the effect structure can be recovered despite strong noise, although the recovered effect is again strongly biased (due to the variance/bias tradeoff).

Spatial vs. temporal deconvolution

Many researchers use ICA to decompose the EEG signal into maximally independent source signals. Because ICA is believed to isolate the signal contributions of individual neural sources, it can be understood as performing a *spatial* deconvolution of the signal. Other source space estimations can also been seen as spatial deconvolutions. Nevertheless, the activity time courses of each independent source may still overlap in time, e.g. due to repeated stimulus presentations. In order to also allow for a *temporal* deconvolution of the signal, *unfold* allows to run the deconvolution not only on the raw EEG signal, but also on independent component activation. This is done by adding a flag (‘`ica`’, ‘`true`’) when fitting the model. Possibly, the prior spatial decomposition of the signal with ICA may improve the performance and interpretability of the final, temporally deconvolved signals.

Figure 8

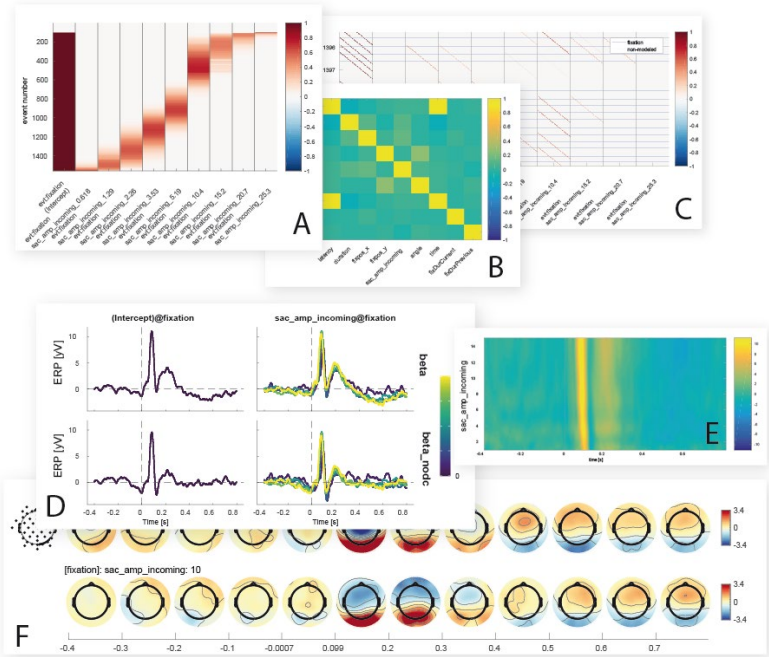

Figure 8. Inbuild data visualization options. Shown are some of the figures currently produced by the *unfold* toolbox. While setting up the model, it is possible to visualize intermediate steps of the analysis, such as the design matrix (A) covariance matrix of the predictors (B) or the time-expanded design matrix (C). After the model is computed, the beta coefficients for one or more predictors can be plotted as ERP-like waveforms with a comparison of with and without deconvolution (D), as erpimages with time against predictor value and color-coded amplitude (E), or as topographical time series (F).

Comparison to a Mass Univariate model (without deconvolution)

The *unfold* toolbox offers the option to compute a mass univariate regression model on the same data using the exact same model but without correction for overlap. In our experience, running this model in addition to the linear deconvolution model can be helpful to understand the impact of overlap on the results. However, with this function, *unfold* can also be used as a

standalone toolbox for Mass-Univariate modeling, for the (rare) cases in which an experiment does not involve any overlapping activity (e.g. from small saccades; Dimigen et al., 2009).

Visualization of results

unfold offers multiple inbuild functions to visualize rERP results. We provide functions for marginal plots over splines and continuous variables, and functions to evaluate splines/continuous covariates at specific values. For the topographical output we make use of functions from the EEGVIS toolbox (Ehinger, 2018).

Exporting the results

unfold focusses on two main things: linear deconvolution and (non)-linear modeling at the single-subject level. In contrast, the toolbox itself does not offer functions for group-level statistics. However, the betas for each participant can be easily exported as plain text (.csv) or as different MATLAB structures to perform statistics with other toolboxes. A tutorial to process *unfold* results using group-level cluster-based permutation tests with the TFCE-toolbox (Mensen & Khatami, 2013) is provided in the online documentation.

A minimal but complete analysis script

The following is a complete analysis script for the hypothetical face/house experiment introduced above (see *Figure 1*). As can be seen, it can be run with a few lines of code.

Box 1. A complete analysis script with *unfold*

```
EEG = pop_load('eeg_example.set') % load dataset into EEGLAB

%% specify models for house/face events & button presses
cfg = []
cfg.formula    = {'y ~ 1 + cat(stim_type) + spl(luminance,10)', 'y ~ 1'}
cfg.eventtypes = {'stimulus_onset', 'button_onset'}

cfg.timelimits = [-0.5, 1]            % time window for response estimation
cfg.channel = 1:64                    % EEG channels to analyze

%% run model & plot results
run('init_unfold.m')                  % start toolbox
EEG = uf_designmat(EEG,cfg)           % create design matrix
EEG = uf_timeexpandDesignmat(EEG,cfg) % time-expand design matrix

EEG = uf_glmfit(EEG,cfg)              % solve regression model

ufresult = uf_condense(EEG)           % reformat results (e.g. for plotting)
uf_plotParam(ufresult,'channel',1)    % visualize rERPs (waveforms/topographies)
```

RESULTS

In this section we validate the *unfold* toolbox based on (1) simulated data and (2) a real dataset from a standard face recognition ERP experiment containing overlapping activities.

Simulated data

To create simulated data, we produced overlapped data using four different response shapes, shown in the first column of Figure 9: (1) a boxcar function, (2) a Dirac delta function, (3) a simulated auditory ERP (the same as used by Lütkenhöner, 2010), and (4) random pink noise. We then simulated 5 s of continuous data, during which 18 experimental events happened. Intervals between subsequent events were randomly drawn from a normal distribution (M = 0.25 s, SD = 0.05 s). Convolving the simulated responses with the randomly generated event latencies produced the continuous overlapped signal depicted in the third column of Figure 9. The last column of Figure 9 shows the non-overlapped responses recovered by *unfold* (orange lines). For comparison, overlapped responses without deconvolution are plotted in dark red. As can be seen, *unfold* recovered the original response in all cases. The data of Figure 1 were also simulated and then analyzed using toolbox. Together, these simulations show conclusively that *unfold* successfully deconvolves heavily overlapping simulated signals.

Figure 9

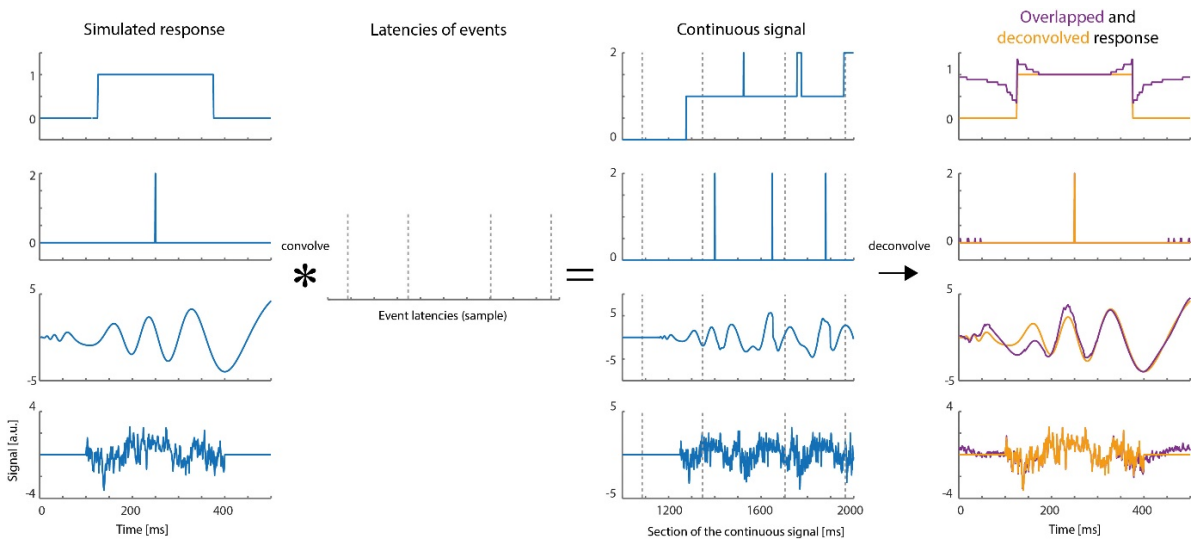

Figure 9. Deconvolution results for simulated signals. Four types of responses (first column: box car, Dirac function, auditory ERP, pink noise) were convolved with random event latencies (second column). A section of the resulting overlapped signal is shown in the third column. The fourth column shows the deconvolved response recovered by the *unfold* toolbox (orange lines). Overlapped responses (without deconvolution) are plotted as violet lines for comparison.

Real data example

Finally, we will also analyze a real dataset from a single participant who performed a standard ERP face discrimination experiment[1]. In this experiment, previously described in the supplementary materials of Dimigen et al. (2009), participants were shown 120 different color images of human faces (7.5° × 8.5°) with a happy, angry, or neutral expression. Their task was to categorize the emotion of the presented face as quickly as possible using three response buttons, operated with the index, middle, and ring finger of the right hand. Each stimulus was presented for 1350 ms. The participant's mean RT was 836 ms.

Although a central fixation cross was presented prior to each trial and participants were instructed to avoid eye movements during the task, concurrent video-based eye-tracking revealed that participants executed at least one involuntary (micro)saccades during the vast majority of trials (see also Dimigen et al., 2009; Yuval-Greenberg et al., 2008). For the participant analyzed here, the median amplitude of these small saccades was 0.6° and most were aimed at the mouth region of the presented faces, which was most informative for the emotion discrimination task.

This means that our stimulus-locked ERPs are contaminated with two other processes: visually-evoked potentials (lambda waves) generated by the retinal image motion produced by the (micro)saccades (Gaarder et al., 1964; Dimigen et al., 2009) and motor processes related to preparing and executing the finger movement.

[1] The same example data was also analyzed in our accompanying paper (Dimigen & Ehinger, 2018), but with a different focus. Further details on this dataset are given in Dimigen (2009) or Dimigen & Ehinger (2018).

Figure 10

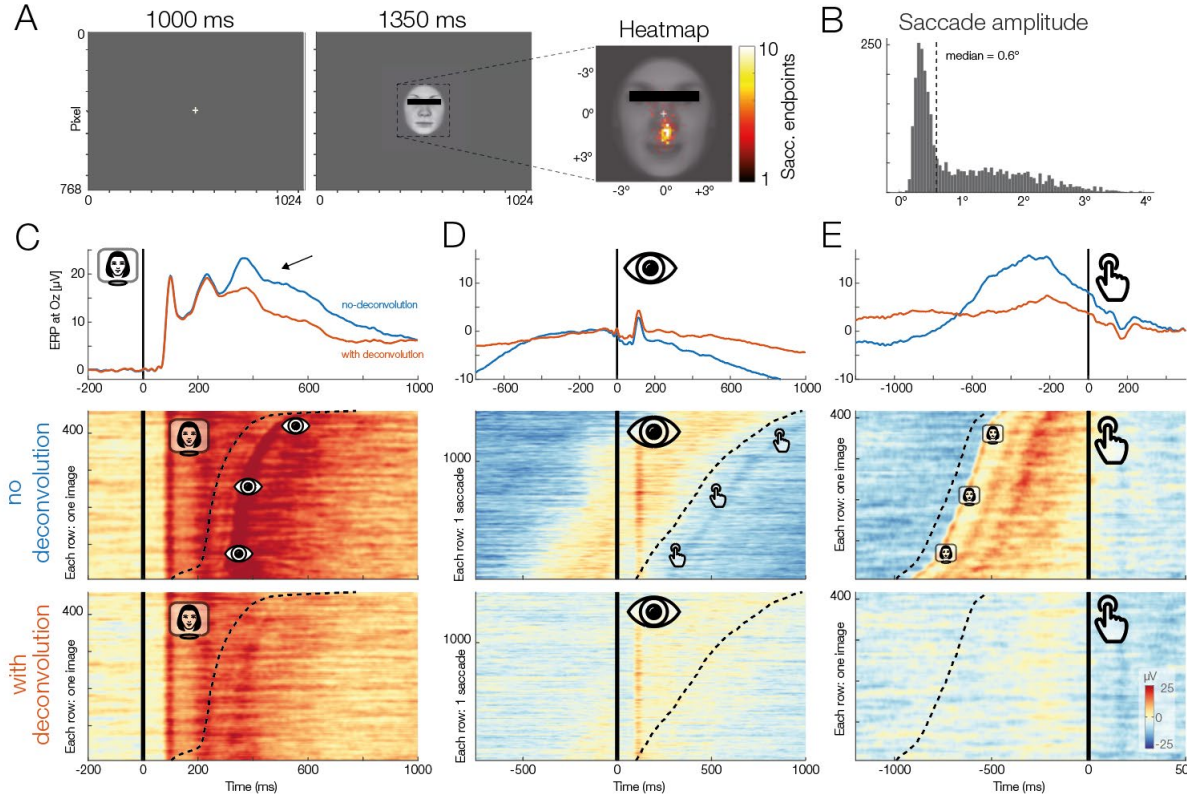

Figure 10. (A) Panel adapted from Dimigen & Ehinger (2018). The participant was shown a stimulus for 1350 ms. (B) The subject was instructed to keep fixation, but as the heatmap shown, made many small involuntary saccades towards the mouth region of the presented stimuli. Each saccade also elicits a visually-evoked response (lambda waves). (C to E) Latency-sorted and color-coded single-trial potentials at electrode Oz over visual cortex (second row) reveal that the vast majority of trials contain not only the neural response to the face (left column), but also hidden visual potentials evoked by involuntary microsaccades (middle column) as well as motor potentials from preparing the button press (right column). Deconvolution modeling with unfold allows us to isolate and remove these different signal contributions (third row), resulting in corrected ERP waveforms for each process (blue vs. red waveforms, top row). This reveals for example that a significant part of the P300 evoked by faces (arrow in top left panel) is really due to microsaccades and button presses and not the stimulus presentation. Data and code to reproduce the figure can be found under https://osf.io/wbz7x/.

To disentangle these potentials with *unfold*, we specified three events: Stimulus onset, saccade onset, and button press. For this simple demonstration, we modeled both stimulus onsets and button press events using only an intercept term (y~1), that is regardless of emotion. For the saccade onsets, we included both an intercept as well as saccade amplitude as a continuous predictor, because larger saccades are followed by larger lambda waves (e.g. Gaarder et al., 1964; Dimigen et al., 2009). Because this relationship is non-linear (e.g. Dandekar et al., 2012) we used a set of 10 splines in the formula, `y ~ 1 + spl(saccade_amplitude,10)`. Brain responses were modeled in the time window from -1.5 s to 1 s around each event. Before fitting the model, we removed all intervals from the design matrix in which the recorded activity at any channels differed by > 250 µV within a 2 s

Figure 10 presents the results for occipital electrode Oz and the signal both without (in red) and without (blue) the modeling and removal of overlapping activity. The large effect of overlapping activity can be clearly seen in the averaged ERP waveforms (top row in panels C, D, and E). In the corresponding panels below that, we see the color-coded single trial activity (*erpimages*), in which segments time-locked to one type of event (e.g. stimulus onset) were sorted by the latency of the temporally adjacent event (e.g. saccade onset). These panels clearly show the overlapping activity and how it was successfully removed by the deconvolution. In particular, we wish to highlight the substantial effect of overlap correction on the shape of both the stimulus-onset ERP (elicited by the faces) and the response-related ERP (elicited by the button press), despite the fact that average RT was relatively long (> 800 ms) in this task. Microsaccades have an additional distorting effect (Dimigen et al., 2009). We can therefore easily imagine how without any overlap correction, differences in mean RT and microsaccade occurrence between condition will create spurious condition effects in the stimulus-ERP. A more complex application where we correct for similar spurious effects in a natural reading EEG experiment with 48 participants is found in Dimigen & Ehinger (2018).

DISCUSSION

Human behavior in natural environments is characterized by complex motor actions and quasi-continuous, multisensory stimulation. Brain signals recorded under such conditions are characterized by overlapping activity evoked by different processes and typically also influenced by a host of confounding variables that are difficult or impossible to orthogonalize under quasi-experimental conditions. However, even in traditional, highly controlled laboratory experiments, it is often unrealistic to match all stimulus properties between conditions, in particular if the stimuli are high-dimensional, such as words (e.g. word length, lexical frequency, orthographic neighborhood size, semantic richness, number of meanings etc.) or faces (e.g., luminance, contrast, power spectrum, size, gender, age, facial expression, familiarity etc.). In addition, as we demonstrate here, even simple EEG experiments often contain overlapping neural responses from multiple different processes such as stimulus onsets, eye movements, or button presses. Deconvolution modeling allows us to disentangle and isolate these different influences to improve our understanding of the data.

In this article, we presented *unfold*, which deconvolves overlapping potentials and controls for linear or non-linear influences of covariates on the EEG. In the following, we will

discuss in more detail the assumptions, possibilities, and existing limitations of this approach as well as current and future applications.

Where can linear deconvolution be applied?

Linear deconvolution can be applied to many types of paradigms and data. As shown above, one application is to separate stimulus- and response-related components in traditional ERP studies (see also Ouyang et al., 2011, 2015). Deconvolution is also particularly useful with complex ERP designs that involve, for example, multimodal streams of visual, tactile, and auditory stimuli (Spitzer et al., 2016). Deconvolution is also helpful in paradigms where it is problematic to find a neutral interval to place a baseline, for example in experiments with fast tone sequences (Lütkenhöner, 2010). In ERP research, the interval for baseline correction is usually placed immediately before stimulus onset, but activity in this interval can vary systematically between conditions due to overlapping activity, for example in self-paced paradigms (e.g. Ditman, Holcomb, & Kuperberg, 2007). This problem can be solved by deconvolving the signal first and applying the baseline subtraction to the resulting isolated responses.

Time-continuous covariates

It is also possible to add time-continuous signals as predictors to the design matrix (Crosse et al., 2016; Lalor, Pearlmutter, Reilly, McDarby, & Foxe, 2006). Examples for continuous signals that could be added as predictors include the luminance profile of a continuously flickering stimulus (Lalor et al., 2006; VanRullen & MacDonald, 2012), the sound envelope of an audio or speech signal (with temporal lags to model the auditory temporal response function, Crosse, et al., 2016), the participants gaze position or pupil size (from concurrent eye-tracking, see Dimigen & Ehinger, 2018), but also more abstract time series, such as predictions from a cognitive computational model. Including time-continuous covariates such as gait-signals, movement features, or environmental sounds could improve the model fit in mobile EEG situations (Ehinger et al., 2014; Gramann, Jung, Ferris, Lin, & Makeig, 2014).

Underlying assumptions

A fundamental assumption of traditional ERP averaging is that the shape of the underlying neural response is identical in all trials belonging to the same condition. Trials with short and long manual reaction times are therefore usually averaged together. Similarly, with linear deconvolution modeling, we assume that the brain response is the same for all events of

a given type. However, like in traditional ERP analyses, we also assume that the neural response is independent of the interval between two subsequent events (e.g. the interval between a stimulus and a manual response). This is likely a strong simplification, since neural activity will likely differ between trials with a slow or fast reaction.

A related assumption concerns sequences of events: Processing one stimulus can change the processing of a following stimulus, for instance due to adaptation, priming, or other attentional effects. We want to note that if such sequential effects occur often enough in an experiment, they can be explicitly modeled; for example, on could add an additional predictors coding whether a stimulus is repeated or not or whether it occurred early or late in a sequence of stimuli. We hope that the *unfold* toolbox will facilitate the analysis of simulations on these issues and also propose to analyze experiments where temporal overlap is experimentally varied.

Modeling nonlinear effects

Nonlinear predictors can have considerable advantages over linear predictors. However, one issue that is currently unresolved is how to select an appropriate number of spline functions to model a nonlinear effect without under- or overfitting the data. While automatic selection methods exist (e.g. based on generalized cross-validation, Wood, 2017), their high computational cost precluded us from using these techniques. In the current implementation of *unfold*, we assume the same number of splines are needed for all parts of the response. But it is possible, for example, that with a constant number of splines the baseline interval is overfitted, whereas the true response is underfitted. Therefore, algorithms to find smoothing parameters need to take into account that the amount of smoothing changes throughout the response. Choosing the correct number of splines that neither overfit nor underfit the data is an important question to resolve, and again, we hope that the *unfold* toolbox will facilitate future simulation studies, new algorithms, and new experiments on this issue.

Time-frequency analysis

While all example analyses presented here were done in the time domain, it is also possible to model and deconvolve overlapping time-frequency representations with *unfold*. One simple option is to enter the band-bass filtered and rectified EEG signal into the model; an alternative is to use the full continuous time-frequency representation (Litvak et al., 2013).

Outlook: Integration with linear mixed models

In recent years, linear mixed-effects models (LMM, e.g. Gelman & Hill, 2007) have been slowly superseding traditional models like repeated-measures ANOVA or the two-stage hierarchical approach used here. LMMs allow to model the hierarchical structure of single-subject and group-level data directly and have several other advantages, for example when analyzing unbalanced designs (Baayen, Davidson, & Bates, 2007; Kliegl, 2010). Combining LMMs with linear deconvolution is theoretically possible. The main challenge is that one needs to fit all continuous EEG datasets of all participants at the same time. Thus, currently, the high computational cost of fitting such large models precludes us from taking advantage of mixed models. Nevertheless, recent progress with similarly large models (Wood, Li, Shaddick, & Augustin, 2017) shows that the combination of LMMs with deconvolution modeling might be computationally feasible in future implementations.

Other physiological signals

Finally, it is also possible to model other types of overlapping psychophysiological signals with *unfold*, such as overlapping magnetic fields (MEG, Litvak et al., 2013), pupil dilations (Gagl, Hawelka, & Hutzler, 2011; Wierda, van Rijn, Taatgen, & Martens, 2012) or skin conductance responses (Bach, Flandin, Friston, & Dolan, 2009).

Conclusions

In summary, *unfold* offers an integrated environment to analyze psychophysiological data influenced by overlapping responses, (non)linear covariates, or both. As we show above, this analysis strategy can be beneficial even in case of "traditional", highly-controlled ERP experiments. It also allows us to record EEG data under more natural situations, for example those with unconstrained eye movement behavior, which is typical for the emerging fields of virtual reality and mobile brain/body imaging studies. Applications of *unfold* to free viewing studies can be found in an accompanying paper (Dimigen & Ehinger, 2018). The toolbox is freely available at http://www.unfoldtoolbox.org with tutorials and documentation.

REFERENCES

Amsel, B. D. (2011). Tracking real-time neural activation of conceptual knowledge using single-trial event-related potentials. *Neuropsychologia*, *49*(5), 970–983. http://doi.org/10.1016/j.neuropsychologia.2011.01.003

Baayen, H. R., Davidson, D., & Bates, D. M. (2007). Mixed-effect models R. Harald Baayen. *Linguistics › Miscellaneous Papers*, *59*(4), ? http://doi.org/10.1016/j.jml.2007.12.005

Bach, D. R., Flandin, G., Friston, K. J., & Dolan, R. J. (2009). Time-series analysis for rapid event-related skin conductance responses. *Journal of Neuroscience Methods*, *184*(2), 224–234. http://doi.org/10.1016/j.jneumeth.2009.08.005

Bardy, F., Van Dun, B., Dillon, H., & Cowan, R. (2014). Least-squares (LS) deconvolution of a series of overlapping cortical auditory evoked potentials: A simulation and experimental study. *Journal of Neural Engineering*, *11*(4). http://doi.org/10.1088/1741-2560/11/4/046016

Burns, M. D., Bigdely-Shamlo, N., Smith, N. J., Kreutz-Delgado, K., & Makeig, S. (2013). Comparison of averaging and regression techniques for estimating Event Related Potentials. *Conference Proceedings : ... Annual International Conference of the IEEE Engineering in Medicine and Biology Society. IEEE Engineering in Medicine and Biology Society. Conference*, *2013*, 1680–3. http://doi.org/10.1109/EMBC.2013.6609841

Crosse, M. J., Di Liberto, G. M., Bednar, A., & Lalor, E. C. (2016). The Multivariate Temporal Response Function (mTRF) Toolbox: A MATLAB Toolbox for Relating Neural Signals to Continuous Stimuli. *Frontiers in Human Neuroscience*, *10*. http://doi.org/10.3389/fnhum.2016.00604

Dale, A. M., & Buckner, R. L. (1997). Selective averaging of rapidly presented individual trials using fMRI. *Human Brain Mapping*, *5*(5), 329–340. http://doi.org/10.1002/(SICI)1097-0193(1997)5:5<329::AID-HBM1>3.0.CO;2-5

Dandekar, S., Privitera, C., Carney, T., & Klein, S. A. (2012). Neural saccadic response estimation during natural viewing. *Journal of Neurophysiology*, *107*(6), 1776–1790. http://doi.org/10.1152/jn.00237.2011

De Casteljau, P. (1959). Courbes à pôles. *National Industrial Property Institute (France)*. http://doi.org/10.1.1.86.162

Delgado, R. E., & Ozdamar, O. (2004). Deconvolution of evoked responses obtained at high stimulus rates. *J Acoust Soc Am*, *115*(3), 1242–1251. http://doi.org/10.1121/1.1639327

Delorme, A., & Makeig, S. (2004). EEGLAB: an open sorce toolbox for analysis of single-trail EEG dynamics including independent component anlaysis. *Journal of Neuroscience Methods*, *134*, 9–21. http://doi.org/10.1016/j.jneumeth.2003.10.009

Ditman, T., Holcomb, P. J., & Kuperberg, G. R. (2007). An investigation of concurrent ERP and self-paced reading methodologies. *Psychophysiology*, *44*(6), 927–935. http://doi.org/10.1111/j.1469-8986.2007.00593.x

Ehinger, B. V. (2018). EEGVIS Toolbox. *Https://github.com/behinger/eegvis/*. http://doi.org/10.5281/zenodo.1312813

Ehinger, B. V., Fischer, P., Gert, A. L., Kaufhold, L., Weber, F., Pipa, G., & König, P. (2014). Kinesthetic and vestibular information modulate alpha activity during spatial navigation: a mobile EEG study. *Frontiers in Human Neuroscience*, *8*. http://doi.org/10.3389/fnhum.2014.00071

Eysholdt, U., & Schreiner, C. (1982). Maximum length sequences-a fast method for measuring brain-stem-evoked responses. *Audiology*, *21*, 242–250.

Fong, D. C.-L., & Saunders, M. (2011). LSMR: An Iterative Algorithm for Sparse Least-Squares Problems. *SIAM Journal on Scientific Computing*, *33*(5), 2950–2971. http://doi.org/10.1137/10079687X

Frömer, R., Maier, M., & Abdel Rahman, R. (2018). Group-Level EEG-Processing Pipeline for Flexible Single Trial-Based Analyses Including Linear Mixed Models. *Frontiers in Neuroscience*, *12*. http://doi.org/10.3389/fnins.2018.00048

Gagl, B., Hawelka, S., & Hutzler, F. (2011). Systematic influence of gaze position on pupil size measurement: Analysis and correction. *Behavior Research Methods*, *43*(4), 1171–1181. http://doi.org/10.3758/s13428-011-0109-5

Gelman, A., & Hill, J. (2007). *Data analysis using regression and multilevel/hierarchical models*. *Cambridge*. http://doi.org/10.2277/0521867061

Gramann, K., Jung, T.-P., Ferris, D. P., Lin, C.-T., & Makeig, S. (2014). Toward a new cognitive neuroscience: modeling natural brain dynamics. *Frontiers in Human Neuroscience*, *8*. http://doi.org/10.3389/fnhum.2014.00444

Gramfort, A., Luessi, M., Larson, E., Engemann, D. A., Strohmeier, D., Brodbeck, C., … Hämäläinen, M. S. (2014). MNE software for processing MEG and EEG data. *NeuroImage*, *86*, 446–460.

http://doi.org/10.1016/j.neuroimage.2013.10.027

Halliday, A. (1982). The visual evoked potentials in healthy subjects. In *Evoked potentials in clinical testing* (pp. 57–113). London: Churghill Livingstone.

Hanke, M., & Halchenko, Y. O. (2011). Neuroscience Runs on GNU/Linux. *Frontiers in Neuroinformatics*, *5*. http://doi.org/10.3389/fninf.2011.00008

Hansen, J. C. (1983). Separation of overlapping waveforms having known temporal distributions. *Journal of Neuroscience Methods*, *9*(2), 127–139. http://doi.org/10.1016/0165-0270(83)90126-7

Hauk, O., Davis, M. H., Ford, M., Pulvermüller, F., & Marslen-Wilson, W. D. (2006). The time course of visual word recognition as revealed by linear regression analysis of ERP data. *NeuroImage*, *30*(4), 1383–1400. http://doi.org/10.1016/j.neuroimage.2005.11.048

Jewett, D. L., Caplovitz, G., Baird, B., Trumpis, M., Olson, M. P., & Larson-Prior, L. J. (2004). The use of QSD (q-sequence deconvolution) to recover superposed, transient evoked-responses. *Clinical Neurophysiology*, *115*(12), 2754–2775. http://doi.org/10.1016/j.clinph.2004.06.014

Kliegl. (2010). Experimental effects and individual differences in linear mixed models: estimating the relationship between spatial, object, and attraction effects in visual attention. *Frontiers in Psychology*, *1*(1). http://doi.org/10.3389/fpsyg.2010.00238

Kristensen, E., Guerin-Dugué, A., & Rivet, B. (2017). Regularization and a general linear model for event-related potential estimation. *Behavior Research Methods*, *49*(6), 2255–2274. http://doi.org/10.3758/s13428-017-0856-z

Kristensen, E., Rivet, B., & Guérin-Dugué, A. (2017). Estimation of overlapped Eye Fixation Related Potentials: The General Linear Model, a more flexible framework than the ADJAR algorithm. *Journal of Eye Movement Research*, *10*(1), 1–27. http://doi.org/10.16910/JEMR.10.1.7

Lalor, E. C., Pearlmutter, B. A., Reilly, R. B., McDarby, G., & Foxe, J. J. (2006). The VESPA: A method for the rapid estimation of a visual evoked potential. *NeuroImage*, *32*(4), 1549–1561. http://doi.org/10.1016/j.neuroimage.2006.05.054

Litvak, V., Jha, A., Flandin, G., & Friston, K. (2013). Convolution models for induced electromagnetic responses. *NeuroImage*, *64*(1), 388–398. http://doi.org/10.1016/j.neuroimage.2012.09.014

Lopez-Calderon, J., & Luck, S. J. (2014). ERPLAB: an open-source toolbox for the analysis of event-related potentials. *Frontiers in Human Neuroscience*, *8*. http://doi.org/10.3389/fnhum.2014.00213

Luong, B. (2016). Free-knot spline approximation.

Lütkenhöner, B. (2010). Baseline correction of overlapping event-related responses using a linear deconvolution technique. *NeuroImage*, *52*(1), 86–96. http://doi.org/10.1016/j.neuroimage.2010.03.053

Marsh, R. R. (1992). Signal to Noise Constraints on maximum length sequence auditory Brain-Stem Responses. *Ear and Hearing*, *13*(6), 396–400. http://doi.org/10.1097/00003446-199212000-00004

Mensen, A., & Khatami, R. (2013). Advanced EEG analysis using threshold-free cluster-enhancement and non-parametric statistics. *NeuroImage*, *67*, 111–118. http://doi.org/10.1016/j.neuroimage.2012.10.027

Oostenveld, R., Fries, P., Maris, E., & Schoffelen, J.-M. (2011). FieldTrip: Open source software for advanced analysis of MEG, EEG, and invasive electrophysiological data. *Computational Intelligence and Neuroscience*, *2011*, 1–10. http://doi.org/10.1155/2011/156869

Ouyang, G., Herzmann, G., Zhou, C., & Sommer, W. (2011). Residue iteration decomposition (RIDE): A new method to separate ERP components on the basis of latency variability in single trials. *Psychophysiology*, *48*(12), 1631–1647. http://doi.org/10.1111/j.1469-8986.2011.01269.x

Ouyang, G., Sommer, W., & Zhou, C. (2015). A toolbox for residue iteration decomposition (RIDE)-A method for the decomposition, reconstruction, and single trial analysis of event related potentials. *Journal of Neuroscience Methods*, *250*, 7–21. http://doi.org/10.1016/j.jneumeth.2014.10.009

Penny, W., Friston, K., Ashburner, J., Kiebel, S., & Nichols, T. (2006). *Statistical Parametric Mapping: The Analysis of Functional Brain Images: The Analysis of Functional Brain Images*. *Statistical Parametric Mapping The Analysis of Functional Brain Images* (Vol. 8). http://doi.org/10.1016/B978-012372560-8/50002-4

Pernet, C. R., Chauveau, N., Gaspar, C., & Rousselet, G. A. (2011). LIMO EEG: A toolbox for hierarchical linear modeling

of electroencephalographic data. *Computational Intelligence and Neuroscience*, *2011*. http://doi.org/10.1155/2011/831409

Qian, J., Hastie, T., Friedman, J., Tibshirani, R., & Simon, N. (2013). Glmnet for Matlab. *URL Http://www. Stanford. Edu/~ Hastie/glmnet_matlab*.

Runge, C. (1901). Über empirische Funktionen und die Interpolation zwischen äquidistanten Ordinaten. *Zeitschrift Für Mathematik Und Physik*, *46*, 224–243.

Smith, N. J. (2013). pyrERP.

Smith, N. J., & Kutas, M. (2015a). Regression-based estimation of ERP waveforms: I. The rERP framework. *Psychophysiology*, *52*(2), 157–168. http://doi.org/10.1111/psyp.12317

Smith, N. J., & Kutas, M. (2015b). Regression-based estimation of ERP waveforms: II. Nonlinear effects, overlap correction, and practical considerations. *Psychophysiology*, *52*(2), 169–181. http://doi.org/10.1111/psyp.12320

Smith, S. M., & Nichols, T. E. (2009). Threshold-free cluster enhancement: Addressing problems of smoothing, threshold dependence and localisation in cluster inference. *NeuroImage*, *44*(1), 83–98. http://doi.org/10.1016/j.neuroimage.2008.03.061

Spitzer, B., Blankenburg, F., & Summerfield, C. (2016). Rhythmic gain control during supramodal integration of approximate number. *NeuroImage*, *129*, 470–479. http://doi.org/10.1016/j.neuroimage.2015.12.024

Talsma, D., & Woldorff, M. G. (2004). Methods for the Estimation and Removal of Artifacts and Overlap in ERP Waveforms. In T. Handy (Ed.), *Event-related potentials: A methods handbook.* Cognitive Psychology, Clinical Neuropsychology. http://doi.org/10.1212/01.wnl.0000217365.45426.9a

Van Humbeeck, N., Meghanathan, R. N., Wagemans, J., van Leeuwen, C., & Nikolaev, A. R. (2018). Presaccadic EEG activity predicts visual saliency in free-viewing contour integration. *Psychophysiology*, e13267. http://doi.org/10.1111/psyp.13267

VanRullen, R., & MacDonald, J. S. P. (2012). Perceptual echoes at 10 Hz in the human brain. *Current Biology*, *22*(11), 995–999. http://doi.org/10.1016/j.cub.2012.03.050

Wang, T., Özdamar, Ö., Bohórquez, J., Shen, Q., & Cheour, M. (2006). Wiener filter deconvolution of overlapping evoked potentials. *Journal of Neuroscience Methods*, *158*(2), 260–270. http://doi.org/10.1016/j.jneumeth.2006.05.023

Wierda, S. M., van Rijn, H., Taatgen, N. A., & Martens, S. (2012). Pupil dilation deconvolution reveals the dynamics of attention at high temporal resolution. *Proceedings of the National Academy of Sciences*, *109*(22), 8456–8460. http://doi.org/10.1073/pnas.1201858109

Wilkinson, G. N., & Rogers, C. E. (1973). Symbolic Description of Factorial Models for Analysis of Variance. *Applied Statistics*, *22*(3), 392. http://doi.org/10.2307/2346786

Woldorff, M. G. (1993). Distortion of ERP averages due to overlap from temporally adjacent ERPs: Analysis and correction. *Psychophysiology*, *30*(1), 98–119. http://doi.org/10.1111/j.1469-8986.1993.tb03209.x

Wood, S. N. (2017). Generalized additive models : an introduction with R. *Texts in Statistical Science*, xvii, 392 . http://doi.org/10.1111/j.1541-0420.2007.00905_3.x

Wood, S. N., Li, Z., Shaddick, G., & Augustin, N. H. (2017). Generalized Additive Models for Gigadata: Modeling the U.K. Black Smoke Network Daily Data. *Journal of the American Statistical Association*, *112*(519), 1199–1210. http://doi.org/10.1080/01621459.2016.1195744

Zhang, J. (1998). Decomposing stimulus and response component waveforms in ERP. *Journal of Neuroscience Methods*, *80*(1), 49–63. http://doi.org/10.1016/S0165-0270(97)00194-5